Orbital Dimerization and Dynamic Jahn-Teller Effect in NaTiSi$_2$O$_6$

M. J. Konstantinović [a,*], J. van den Brink, [b] Z. V. Popović [a,c,**], V. V. Moshchalkov [a], M. Isobe [d], and Y. Ueda [d]

[a] *Laboratorium voor Vaste-Stoffysica en Magnetisme,*
Katholieke Universiteit Leuven, Celestijnenlaan 200D, B-3001 Leuven, Belgium
[b] *Institut-Lorentz for Theoretical Physics, Universiteit Leiden,*
P.O. Box 9506, 2300 RA Leiden and Faculty of Applied Physics,
University of Twente, P.O. Box 217, 7500 AE Enschede, The Netherlands
[c] *Institute of Physics-Belgrade, P. O. Box 68, 11080 Belgrade/Zemun, Yugoslavia and*
[d] *Institute for Solid State Physics, The University of Tokyo,*
5-1-5 Kashiwanoha, Kashiwa, Chiba 277-8581, Japan

We study with Raman scattering technique two types of phase transitions in the pyroxene compounds NaMSi$_2$O$_6$ (with M=Ti, V, and Cr). In the quasi one-dimensional S=1/2 system NaTiSi$_2$O$_6$ we observe anomalous high-temperature phonon broadening and large changes of the phonon energies and line-widths across the phase transition at 210 K. The phonon anomalies originate from an orbital order-disorder phase transition and these results –combined with theoretical considerations– indicate that the high temperature dynamical Jahn-Teller phase of NaTiSi$_2$O$_6$ exhibits a spontaneous breaking of translational symmetry into a dimerized, Jahn-Teller distorted, orbital ordered state under the formation of spin valence bonds. In S=1 NaVSi$_2$O$_6$ orbital degrees of freedom are strongly suppressed and the magnetic excitations are well described within a Heisenberg model, indicating that at T$_N$=19K this system orders antiferromagnetically.

Introduction. Electrons in strongly correlated transition-metal compounds can be regarded as having separate spin, charge and orbital degrees of freedom. It is the interplay between these, combined with their coupling to the lattice, that gives rise to a wealth of possible spin, charge and orbital orderings, as observed for instance in many Colossal Magneto-Resistance manganites [1], cuprates [2], titanates (e.g. LaTiO$_3$ [3]) and vanadates (e.g. V$_2$O$_3$ [4] and LiVO$_2$ [5]).

Systems with orbital degeneracy are particularly interesting because orbitals couple to the lattice via the cooperative Jahn-Teller (JT) effect on one hand, and via superexchange interactions to the electronic spin on the other hand [2]. Therefore at an orbital ordering phase transition the magnetic susceptibility and phonon properties will be affected at the same time. Experimentally, however, such an interrelation is seldom found: in general the dominant JT orbital-lattice coupling obscures the more subtle effects due to the superexchange.

Pyroxenes are large family of compounds (AMB$_2$O$_6$; A=alkali-metal, M=transition-metal, and B=Si, Ge) which structure consists of isolated quasi one-dimensional chains of edge-sharing MO$_6$ octahedra, linked together by the corner-sharing BO$_4$ tetrahedra, Fig. 1. Particularly, the compounds with *active t$_{2g}$* orbitals (M=Ti,V, and Cr) are expected to have electronic interactions governed by both orbital degeneracy and anisotropy. Interestingly, the sodium-silicon system with titanium, NaTiSi$_2$O$_6$, is rather different from other pyroxenes as it lacks low-temperature AF order, and shows signs of the opening of a spin gap instead [6, 7, 8, 15]. Ti^{3+} corresponds to S=1/2, and since all Ti ions are in equivalent crystallographic positions, this material is a prime candidate to show a spin-Peierls (SP) phase transition. Indeed, its magnetic susceptibility [6] sharply decreases below 210 K, indicating a transition to a spin-singlet state, which could in principle be of the SP type. But already the high-temperature magnetic susceptibility data does not support such a SP scenario, since the phase transition occurs at a temperature that is higher then the maximum point of the Bonner-Fisher curve, which implies that the transition cannot solely be driven by magnetic fluctuations [6]. Based on structural analysis, Isobe et.al. anticipated that orbital dimerization might be responsible for such behavior [6].

In this Letter, we report a Raman scattering study on a family of pyroxene compounds from which we conclude that orbital degrees of freedom play decisive role in physical properties of NaTiSi$_2$O$_6$, and that NaTiSi$_2$O$_6$ undergoes an orbital order phase transition at T$_{OO}$=210 K. At high temperatures the fluctuations of the orbital degrees of freedom lead to a dynamic Jahn-Teller phase with anomalous phonon broadening and remnant antiferromagnetic (AF) spin fluctuations. We find that the dramatic drop of the magnetic susceptibility below T$_{OO}$ is accompanied with a structural change, just as one would expect for a canonical orbital ordering transition. These results, combined with the microscopic orbital-spin model that we derive, suggest that the quasi one-dimensional dynamical Jahn-Teller phase of NaTiSi$_2$O$_6$ exhibits a spontaneous breaking of the translational symmetry into an dimerized orbital ordered state with a spin gap due to the formation of spin valence bonds. The paper is organized as follows: first we present the Raman spectra and underline important observations, then we discuss the electronic structure of pyroxenes and derive a microscopic model. Finally, we demonstrate that all observed effects (including susceptibility data) can be
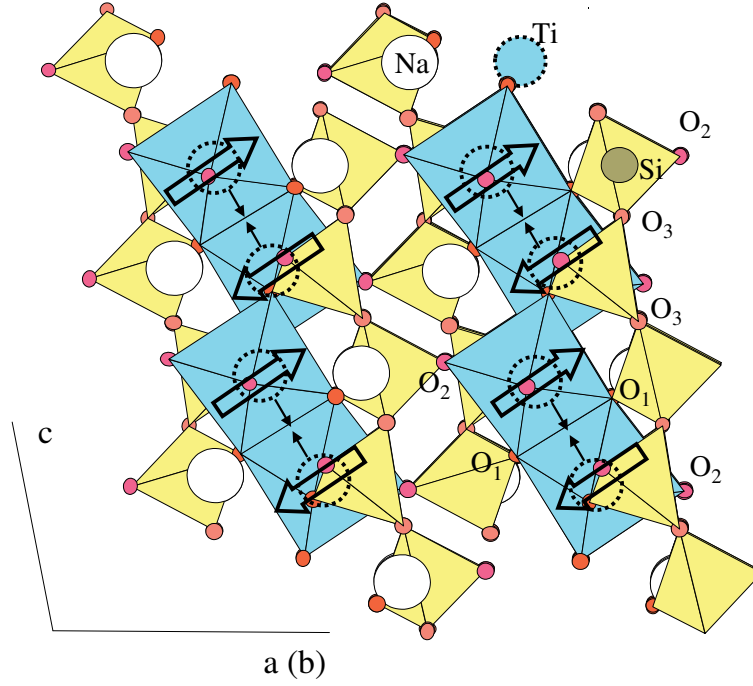
FIG. 1: a) Crystal structure of $NaTiSi_2O_6$. Block arrows denote magnetic moments, and small arrows represent possible distortions (dimerization) of the TiO_6 octahedra in the low temperature phase.

accounted by our model.

Experiment. High-quality powder samples of $NaMSi_2O_6$ (M=Ti, V, and Cr) were prepared by a solid-state reaction of mixtures with an appropriate molar ratio of $Na_2MSi_4O_{11}$, M and MO_2. Details of the sample preparation are published elsewhere [6]. Raman spectra are measured in the backscattering configuration, using 514.5 nm line of an Ar-ion laser, micro-Raman system with a DILOR triple monochromator, and a liquid nitrogen cooled charge-coupled device detector. For the low-temperature measurements we used the Oxford continuous-flow cryostat with a 0.5 mm thick window. The focusing of the laser beam is realized with a long distance (10 mm focal length) microscope objective (magnification 50×).

The pyroxenes crystallize in a monoclinic unit cell with the space group $C2/c$ [9]. The unit cell consists of four formula units (Z=4) with 40 atoms in all. The site symmetry of Na, M, Si, O_1, O_2 and O_3 atoms are (4e), (4e), (8f), (8f), (8f) and (8f), respectively. Thus, the factor-group-analysis (FGA) yields: (Na, M)(C_2) $\Gamma = A_g + A_u + 2B_{1g} + 2B_u$; (Si, O_1, O_2, O_3)(C_1) $\Gamma = 3A_g + 3A_u + 3B_g + 3B_u$. Summarizing these representations and subtracting the acoustic modes $(A_u + 2B_u)$, we obtain the following irreducible representations of $NaMSi_2O_6$ vibrational modes:

$$\begin{aligned}
\Gamma_{NaMSi_2O_6}^{opt.} &= 14A_g(xx, yy, zz, xz) + 16B_g(xy, yz) \\
&+ 13A_u(\mathbf{E}||\mathbf{y}) + 14B_u(\mathbf{E}||\mathbf{x}, \mathbf{E}||\mathbf{z})
\end{aligned}$$

The unpolarized Raman spectra of $NaMSi_2O_6$ (M=Ti, V, Cr) are shown in Fig. 2. At the room temperature we find around 30 phonon modes as predicted by FGA. The Raman spectra of different compounds are similar as expected for isostructural materials, and the phonon modes can be crudely grouped into two energy regions. The modes in the spectral range below 500 cm^{-1} originate from the bond bending vibrations, whereas the higher frequency modes originate from the stretching vibrations. The highest energy modes are mainly due to the non-bridging Si-O ion vibrations, because of the shortest Si-O tetrahedral bonds. The modes of NaMSi2O6 at 1055/1032 cm^{-1} (Cr), 1042/1025 cm^{-1} (V), and 1042/1025 cm^{-1} (Ti), represent Si-O_2 (see Fig. 2) antisymmetric/symmetric bond stretching vibrations, respectively. Their frequency difference scales as R^{-3} in a full accordance with difference between Si-O_2 bond lengths in these materials. Similarly, the modes at 990/967 cm^{-1} (Cr), 972/954 cm^{-1} (V), and 965 cm^{-1}(Ti), we assign as antisymmetric/symmetric pairs of Si-O_1 bond stretching modes. This simplified mode assignment becomes inapplicable at lower frequencies due to more complicated normal coordinates of corresponding vibrations. However, besides similarities, we also observe two very important effects. First, most of *the phonon line widths are dramatically increasing in the components with smaller spin values* $(V^{3+} \rightarrow S = 1, Cr^{3+} \rightarrow S = 3/2)$. Second, the spectra of $NaTiSi_2O_6$, due to the large phonon broadening, show effectively less phonon modes then expected by FGA, and observed in other pyroxenes. The latter effect may also be regarded as a consequence of a high temperature "*higher*
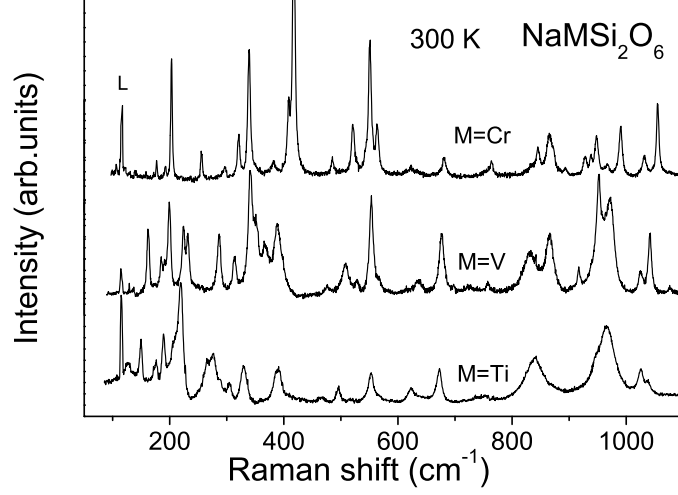
FIG. 2: Raman spectra of NaMSi$_2$O$_6$.

symmetry lattice state" of NaTiSi$_2$O$_6$.

By lowering the temperature we find a dramatic change in the phonon Raman spectra of NaTiSi$_2$O$_6$ around 210 K, see Fig. 3a,b. The modes at 221 and 209 cm^{-1} exhibit the anti-crossing behavior, see inset Fig.3a, which indicates that these two modes belong to the same symmetry class below T_c. A similar effect is observed for all other such pair of modes (one more pair is also visible in Fig. 3a at about 180 and 190 cm^{-1}) in the spectra, which suggests that in the low-T phase of NaTiSi$_2$O$_6$ all Raman active modes are of the same (A_g) symmetry type. Furthermore, our reflectance measurements (will be published separately, Ref. [10]) show that the infrared active phonon modes can be distinguished from the Raman modes, since the center of inversion remains to be the symmetry element in the low-T phase. Accordingly, we uniquely determine the space group of the low-T phase of NaTiSi$_2$O$_6$ to be P$\bar{1}$. *This space group requires the translation symmetry breaking of the TiO$_6$ chain* (the tentative distortion pattern of the low-T phase is shown in Fig. 1) which is in agreement with preliminary X-ray diffraction and neutron scattering data [11].

Moreover, we show in details the temperature dependence of the structure around 970 cm^{-1}, Fig. 3b. The mode at about 946 cm^{-1} softens by about 10 cm^{-1}, while mode at 966 cm^{-1} "splits", and hardens by 25 cm^{-1}, see inset in Fig. 3b. The full width at half maximum (FWHM) of the 946 cm^{-1} (circles) and 966 cm^{-1} (squares) phonons (the FWHM is estimated from Lorenzian-fit) increase up to the maximum value at about 210 K, and then decreases to the saturation value which is much smaller then the T=300 K value, see right inset of Fig. 3b. In fact, all Raman-active phonons exhibit anomalies at the temperature which coincides with T_c obtained from susceptibility measurements [6] indicating that *the magnetic ordering is accompanied with the structural phase transition* just as one would expect for an canonical orbital-ordering transition. Besides, behavior of FWHM implies that *the bond fluctuations are considerably larger in the high-T then in low-T phase*(proximity of the structural phase transition induces the largest fluctuations, producing the maximum FWHM at T$_{OO}$). Due to the JT effect bond fluctuations emphasize the strong orbital character of disorder above the phase transition temperature[12, 13].

Contrary to S=1/2 compound, in the low temperature Raman spectra of NaVSi$_2$O$_6$, see Fig. 3c, we did not observe the phonon anomalies. Instead, at low temperatures, broad asymmetric features, typical for the two-magnon excitations in Heisenberg AF ($H = \sum_{i,j} J_{i,j} \mathbf{S}_i \cdot \mathbf{S}_j, J_{i,j} > 0$), appear around 260 and 400 cm^{-1}. According to the linear Anderson's approximation, differential cross section for the two-magnon (tm) Raman scattering is proportional to the two-magnon density of states (DOS), $I_{tm} \sim \sum_{\mathbf{k}} \delta(\omega - 2\omega(\mathbf{k}))$. The dispersion relation is obtained assuming two-dimensional magnetic structure with different exchange interactions along the chains (J$_\parallel$), and perpendicular (J$_\perp$) to the chains: $\omega(\mathbf{k}) = 2S\sqrt{(J_\parallel + J_\perp)^2 - (J_\parallel cos(ka) + J_\perp cos(kb))^2}$. The calculated two-magnon DOS is shown in top panel of Fig. 3c. Two singularities at energies of about 260 and 390 cm^{-1} are obtained for J$_\parallel$ = 85 cm^{-1} and J$_\perp$ = 13 cm^{-1} (120 K and 18 K, respectively), in a very good agreement with experiment. The maximum of the susceptibility curve in NaVSi$_2$O$_6$ is at about 100 K [11] (giving $J_\parallel \sim 80$ K [14]) which is in good agreement with our estimation of the J$_\parallel$. Thus, we conclude that *NaVSi$_2$O$_6$ exhibits an AF ordering.* Similar AF phase has been already observed in other S=1 chain compounds LiVGe$_2$O$_6$ [7], and NaVGe$_2$O$_6$ [15].
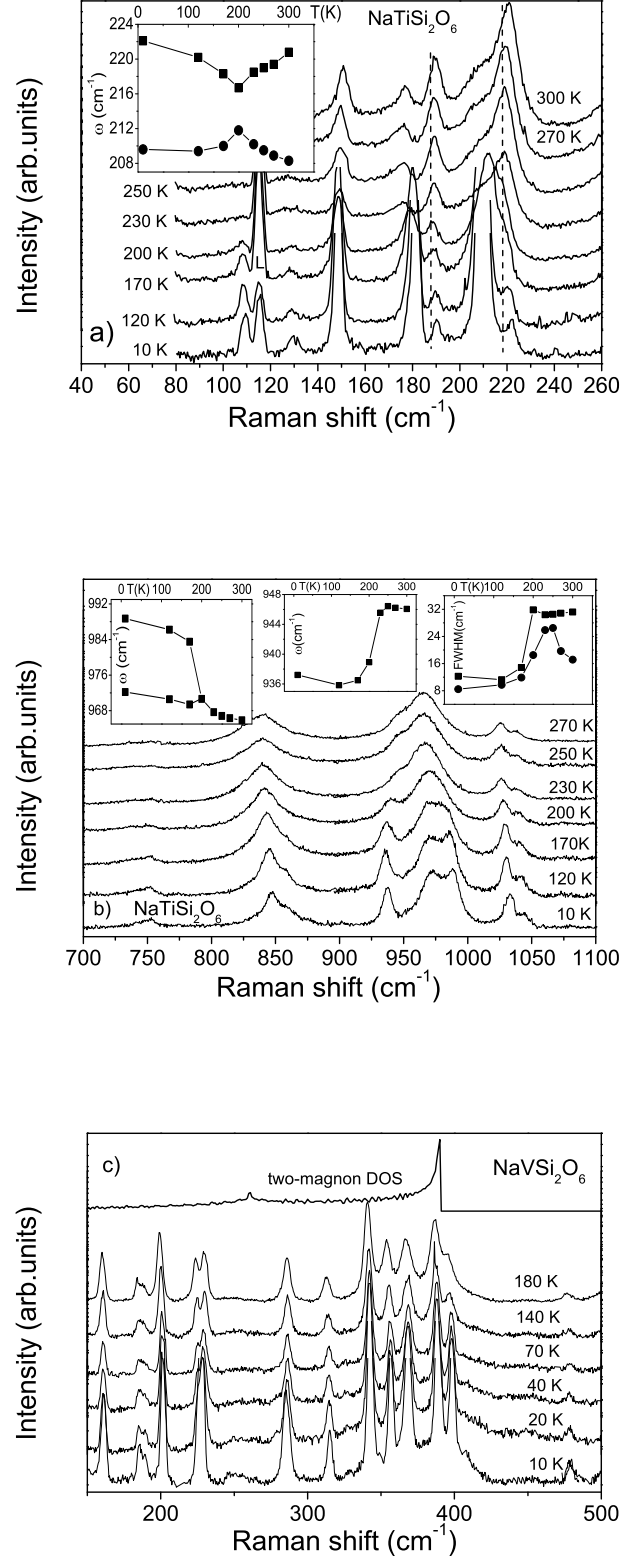
FIG. 3: Temperature dependence of the Raman spectra in a),b) NaTiSi$_2$O$_6$, and c) NaVSi$_2$O$_6$. Top panel in c) shows calculated two-magnon density of states. Insets: Temperature dependencies of the frequency and line width of various phonons in NaTiSi$_2$O$_6$. Vertical dashed line is an guide for the eye.
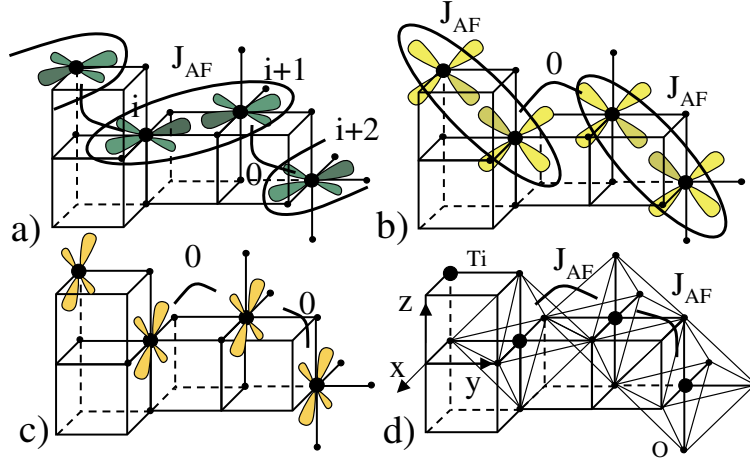
FIG. 4: Schematic presentation of the orbital ordering in NaTiSi$_2$O$_6$. Orbital overlap in a) xy, b) yz, and c) xz planes. d) Heisenberg AF phase.

Pyroxenes: theoretical. Next we discuss the electronic structure. For a single octahedron the cubic crystal field splits the Ti,V or Cr 3d-states into low lying t_{2g} states, with 1,2 or 3 electrons, respectively, and empty states of e_g symmetry at higher energy. The low energy electronic properties are governed by the three-fold degenerate t_{2g} states (the relevant states are $|xy\rangle$, $|yz\rangle$ and $|zx\rangle$) [16].

The Coulomb interaction U between electrons on the same transition metal atoms is large, so the exchange interactions can be determined by a second order perturbation expansion in the electron hopping parameters. The problem is further reduced by considering the symmetry allowed hopping paths in the chain geometry, schematically represented in Fig. 4. If we consider orbitals on two sites in the same xy plane, then only the hopping between $|xy\rangle$ orbitals is relevant (see Fig. 4a). For sites in the yz plane, the $|yz\rangle$ orbitals are relevant, Fig. 4b. In the present geometry (note that x, y, and z in Fig. 4 do not correspond to a, b, and c axis in Fig. 1) there are no transition metal atoms in the same chain that are also in the same xz plane. The $|xz\rangle$ orbitals are therefore non-bonding and can be considered inert on this level of approximation (a tightbinding parametrization [17] shows that other overlap integrals either vanish by symmetry or are more than factor five smaller), see Fig. 4c. For the S=1/2 Titanium system we then obtain the Hamiltonian [18],

$$H^{\mathrm{Ti}} = | \mathrm{J}^{\mathrm{Ti}} | \sum_{i,j} \mathbf{S}_i \cdot \mathbf{S}_j [\frac{1}{4} + T_i^z T_j^z + \frac{(-1)^i}{2}(T_i^z + T_j^z)], \qquad (1)$$

where we use the orbital operators T ($T_i^z = 1/2$ corresponds to an occupied $|xy\rangle$ orbital and $T_i^z = -1/2$ to an occupied $|yz\rangle$ orbital on site i), and i,j are neighboring sites. For the S=1 Vanadium and S=3/2 Chromium system the orbital degree of freedom vanishes ($T = 0$) as the both of the *active* orbitals are occupied, so for the spin system we obtain a simple Heisenberg Hamiltonian $H^{\mathrm{V/Cr}} = | \mathrm{J}^{\mathrm{V/Cr}} | \sum_{i,j} \mathbf{S}_i \cdot \mathbf{S}_j$. This immediately explains the uniqueness of the Ti (S=1/2) system, and the antiferromagnetism in NaVSi$_2$O$_6$ (in fact in all S $\neq$ 1/2 pyroxenes).

Interpretation of experiments. The ground state of Hamiltonian (1), is clearly a *ferro-orbital* state, with spin-singlets on each bond, where the energy per dimer is $-3\mathrm{J}^{\mathrm{Ti}}/4$. The state with all $|xy\rangle$ occupied is degenerate with the state with all $|yz\rangle$ occupied, see Fig. 4. Those states do differ, however, because the dimerization pattern along the chain is shifted by one lattice spacing. At zero temperature the system is condensed in either one of these two dimerized orbital ordered states and the translation symmetry is broken. This explains the structural change at T_c [11], the symmetry change and the energy shifts of the phonon excitations in the Raman spectra of NaTiSi$_2$O$_6$, and the observation of a large spin gap in the susceptibility measurements [6].

At high temperatures, due to strong orbital-lattice coupling and JT effect, the orbital fluctuations produce dramatic effects. Above T$_{\mathrm{OO}}$ the JT distortion disappears: the high-T orbital disordered phase of NaTiSi$_2$O$_6$ may be regarded as an orbital fluctuating phase, and on larger time scales the TiO$_6$ octahedra appear to be undistorted. This causes the crystal to be effectively more symmetric, which is in agreement with the observation of less-then-expected phonon modes in the room temperature Raman spectra. As a consequence, orbital fluctuations induce large phonon broadenings (of course, the modes with Ti-O bonds in their normal coordinates will be mostly affected), as they are indeed found in the room temperature Raman spectra of NaTiSi$_2$O$_6$, see Fig. 2. In that respect the high-T phase of NaTiSi$_2$O$_6$ resembles a *dynamical JT phase* (where the phonon broadening is a signature of the melted static lattice distortions [12, 13]). The spin fluctuations above the orbital ordering temperature [6] can be easily understood in a

straightforward mean-field approximation of Hamiltonian (1), where we can decouple orbitals and spins. If the long range order is absent in the orbital sector, we have for the expectation values $\langle T_i^z \rangle = 0$, and $|\langle T_i^z T_j^z \rangle| < 1/4$, so that the effective exchange constants –and therefore the fluctuations in the spin-sector– are still antiferromagnetic. Thus, the nature of the phase transition in $NaTiSi_2O_6$ can be established: it corresponds to an orbital order-disorder phase transition with appropriate concomitant magnetic and lattice changes.

In the case of two electrons per site ($NaVSi_2O_6$), the orbital fluctuations are strongly suppressed due to inert property of $|xz\rangle$ orbitals, and the corresponding phonon broadenings are much smaller, see Fig. 2. $NaCrSi_2O_6$ has a fully polarized t_{2g} core, no orbital degrees of freedom, and no anomalous phonon broadenings in the Raman spectra.

Conclusions. We report a study of the two types of the phase transitions, observed in pyroxene family, by analyzing the Raman-active phonon and magnon excitations, and their temperature dependence. We find that spin S=1/2 compound, $NaTiSi_2O_6$, exhibits a transition at about 210 K that we assign to be an orbital order-disorder phase transition. It originates from the instability of the high temperature orbital fluctuating - dynamical Jahn-Teller phase, towards a dimerized orbital ordered state, which is accompanied by a lattice distortion and by spin valence bond formation. The spin S=1 system, $NaVSi_2O_6$, on the contrary, does not show this type of instability and orders as a Nèel-type antiferromagnet below $T_N = 19$ K in agreement with our microscopic spin-orbital model for the pyroxenes.

*milan.konstantinovic@fys.kuleuven.ac.be

**Present address: Materials Science Institut, University of Valencia, Poligono La Coma, 46980 Paterna (Valencia), Spain

---

[1] M. Imada, A. Fujimori, and Y. Tokura, Rev. Mod. Phys. **40**, 1039 (1998); Y. Tokura and N. Nagaosa, Science **288**, 462 (2000).
[2] K. I. Kugel and D. I. Khomskii, Sov. Phys. JETP **37**, 725 (1973); Sov. Phys. Usp. **25**, 232 (1982).
[3] B. Keimer, et al. Phys. Rev. Lett. **85**, 3946 (2000); G. Khaliullin and S. Maekawa., *ibid.* **85**, 3950 (2000).
[4] C. Castellani, C. R. Natoli, and J. Ranninger, Phys. Rev. B **18**, 4945 (1978).
[5] H.F. Pen, et al. Phys. Rev. Lett. **78**, 1323 (1997).
[6] M. Isobe, et al., J. Phys. Soc. Japan. **71**, 1423 (2002).
[7] M. D. Lumsden, et al., Phys. Rev. B. **62**, R9244 (2000).
[8] P. Vonlanthen, et al., Phys. Rev. B **65**, 214413 (2002).
[9] H. Ohashi, T. Fujita, and T. Osawa, J. Jpn. Assoc. Mineral. Petrol. Econ. Geol. **77**, 305 (1982).
[10] Z. V. Popović et.al. in preparation.
[11] E. Ninomiya, et al., Proceeding issue of LT23, Japan, 2002.
[12] V. Dediu, et al., Phys. Rev. Lett. **84**, 4489 (2000).
[13] L. Martín-Carrón and A. de Andres, Eur. Phys. J. B **22**, 11 (2001).
[14] J. C. Bonner and M. E. Fisher, Phys. Rev. A **135**, 640 (1964).
[15] A. N. Vasiliev, et al., JETP Letters **76**, 35 (2002).
[16] The splitting of t_{2g}'s due to non-cubic crystal fields is generally weak and smaller than typical hopping integrals.
[17] W. A. Harrison, Electronic Structure and Properties of Solids, Freeman, San Francisco (1980).
[18] We neglect the weak ferromangetism that results from the Hund's rule exchange.